

Robustness of a universal gate set implementation in transmon systems via Chopped Random Basis optimal control

Hervé Atsè Corti¹, Leonardo Banchi^{2, 3}, Alessandro Cidronali⁴

¹*Department of Information Engineering, University of Pisa, via G. Caruso 16, I-56122 Pisa (PI), Italy*

²*Department of Physics and Astronomy, University of Florence, via G. Sansone 1, I-50019 Sesto Fiorentino (FI), Italy*

³*INFN Sezione di Firenze, via G. Sansone 1, I-50019 Sesto Fiorentino (FI), Italy*

⁴*Department of Information Engineering, University of Florence, via di S. Marta 3, I-50139 Firenze (FI), Italy*

Abstract

We numerically study the implementation of a universal two-qubit gate set, composed of CNOT, Hadamard, phase and $\pi/8$ gates, for transmon-based systems. The control signals to implement such gates are obtained using the Chopped Random Basis optimal control technique, with a target gate infidelity of 10^{-2} . During the optimization processes we account for the leakage toward non-computational states, an important non-ideality affecting transmon qubits. We also test and benchmark the optimal control solutions against the introduction of Gaussian white noise and spectral distortion, two key non-idealities that affect the control signals in transmon systems.

Keywords: Transmon qubit; Qubit optimal control; Quantum gate implementation; Superconducting quantum computing; Chopped Random Basis

1. Introduction

The engineering of a scalable and dependable quantum computational system [1] is strongly tied to the reliable implementation of a universal set of quantum gates [2, 3, 4, 5]. This task should be fulfilled with the highest possible fidelity, regardless of the number of qubits and their architecture [6]. To achieve this goal, it is mandatory to properly master the control of the underlying hardware. Due to extreme operating conditions, non-idealities and constraints imposed on control signals by experimental setups, the control of quantum hardware represents one of the most critical topics in the effective development of quantum computational platforms.

Optimal control theory [3, 4, 5, 7] has had a fundamental role in advancing the techniques used to control this kind of systems. The improvement on systems control relies on the ability to manipulate the quantum hardware with optimized control signals. Among optimal control techniques,

the Chopped RAndom Basis (CRAB) optimization method [8, 9, 10] was found to be particularly effective. CRAB operates a gradient-free minimization of system's cost functional, a compelling feature when gradient calculations are prohibitive. Although gradients of quantum evolution can be explicitly computed in small dimensional systems [11], or directly estimated via measurements on multi-qubit systems [12], an efficiently computable formula for higher dimensional multi-level systems is still missing. The gradient-free approach also has the beneficial side-effect to make the algorithm computationally lighter, with respect to gradient-based counterparts. Furthermore, CRAB and specially its dressed version dCRAB (dressed CRAB) [9] are suited for optimization problems where constraints are imposed on control signals since they can easily be considered without adding extra complications to the algorithm.

Superconducting quantum systems are one of the most promising technologies that could be used to build a scalable quantum computer [13, 14, 15], and

the application of optimal control techniques has shown remarkable benefits in steering these systems toward the desired evolution [16, 17, 18]. In this letter we study the performance of the CRAB optimization method [10, 19] to obtain reliable control signals suitable to implement a universal gate set in transmon systems [20, 21, 15] under realistic imperfections, such as the qubit leakage towards non-computational energy levels. More specifically, we test the algorithm on the CNOT (control-NOT), Hadamard, phase and $\pi/8$ gates, and benchmark the proposed robustness [22, 23, 24] of the solutions. Other optimization methods have been considered in the literature for controlling transmon systems [25, 26, 27], with insightful results, yet the performance of CRAB-based algorithms was an open question. Moreover, we test optimal control solutions against the introduction of Gaussian white noise and spectral distortion, which was not considered in the previous literature. The aforementioned disturbances approximate the degrade of optimal control solutions caused by non-idealities in the control electronics. Our results should be considered as a proof of concept demonstration of the gate implementation performances, for transmon systems controlled by signals defined via CRAB-based optimization methods. In order to master the control of an experimental quantum system, it would be beneficial to directly measure in-hardware the target quantity of the optimization (e.g. the infidelity). Such measurements, if performed carefully within an acceptable time frame, can then be used as feedback for closed-loop optimization techniques (e.g. RedCRAB [10]).

This letter is organized as follows. In Sec. 2 we introduce the mathematical formulation to model the controlled evolution of transmon systems. In Sec. 3 we describe how we set up the optimization process. In Sec. 4 we present an example of optimal control solution that implements a CNOT gate, and test the resilience of the optimal control solutions against noise and spectral distortion. Finally, conclusions are drawn in Sec. 5.

2. Control of Transmon Qubits

The Hamiltonian of a quantum system can be conceptually divided in two parts, the drift Hamiltonian and the control Hamiltonian:

$$\hat{H}(t) = \hat{H}^{\text{drift}} + \sum_{j=1}^N \Gamma_j(t) \hat{H}_j^{\text{control}} , \quad (1)$$

where $\Gamma_j(t)$ are the time-dependent control signals, and N is the number of control parameters.

Optimal control algorithms find the control signal profiles $\Gamma_j(t)$ that steer the system toward the desired evolution. The CRAB optimal control algorithm can be described as follows [8]: firstly, we guess an initial pulse $\Gamma_j^0(t)$ for each control parameter; subsequently, we search for a correction to the initial pulse in the form

$$\Gamma_j(t) = \Gamma_j^{\text{CRAB}}(t) = \Gamma_j^0(t) \cdot G_j(t) . \quad (2)$$

The functions $G_j(t)$ are expressed by a limited amount of spectral components N_c :

$$G_j(t) = \sum_{k=1}^{N_c} c_j^k g_j^k(\omega_j^k t) , \quad (3)$$

where the terms g_j^k represent some basis functions for a Fourier-type series expansion, ω_j^k represent angular frequencies, and c_j^k correspond to the coefficients associated to each basis function [8]. In the CRAB implementation adopted by Qutip Python library [28], the functions g_j^k correspond to sinusoidal and cosinusoidal functions. The core aspect of CRAB, that is, the basis frequencies randomization is performed by Qutip through the following approach:

$$\omega_j^k = k \cdot \frac{2\pi}{T} + r_j^k , \quad (4)$$

where r_j^k are random frequency offsets uniformly distributed over $[-0.5, 0.5)$, and $T = \mathcal{O}(1)$ is the dimensionless time duration of the gate implementation (i.e. the time duration of the control signals) – for transmon systems we may consider time in nanoseconds, so the resulting frequencies are assumed in the GHz regime. With $r_j^k = 0$ (i.e. without the basis frequency randomization) the terms ω_j^k are simply the Fourier harmonics. Qutip’s randomization of basis frequencies is slightly different from the randomization process proposed in the original CRAB paper [8] where the randomization is carried out through the following equation:

$$\omega_j^k = (k + r_j^k) \cdot \frac{2\pi}{T} , \quad (5)$$

in this case r_j^k correspond to dimensionless random numbers. However, despite the differences between the two randomization processes, we expect to have similar optimization results since both are able to create a set of random basis frequencies that can

be used to randomize the basis functions. The randomization of basis functions greatly improves the algorithm convergence, despite causing the loss of the orthonormality condition. CRAB optimization problem consists in finding the optimal coefficients c_j^k that minimize a suitable cost functional, such as the gate infidelity, as we describe in more detail hereinafter. This task is then carried out via direct-search, for example via the Nelder-Mead simplex method [29, 8].

The low-energy Hamiltonian of two-transmon system with tunable coupling (also dubbed “g-mon” [30]), in the interaction picture and after the rotating wave approximation, can be written as a Bose-Hubbard type Hamiltonian [21, 15, 31]:

$$\begin{aligned} \hat{H}_{BH} = \sum_{j=1}^2 & \left[\delta_j(t) \hat{n}_j + \frac{\eta}{2} \hat{n}_j (\hat{n}_j - 1) + \right. \\ & + i(\hat{a}_j e^{i\psi_j(t)} - \hat{a}_j^\dagger e^{-i\psi_j(t)}) F_j(t) \left. + \right. \\ & + g(t)(\hat{a}_1 \hat{a}_2^\dagger + \hat{a}_2 \hat{a}_1^\dagger) \left. \right]. \end{aligned} \quad (6)$$

The operators \hat{n}_j correspond to number operators, and \hat{a}_j (\hat{a}_j^\dagger) correspond to annihilation (creation) operators. The terms $\delta_j(t)$ can be controlled by externally modulating the magnetic flux in each transmon [21], and correspond to the detuning parameters, that is how much the j -th qubit oscillation frequency departs from that of the control resonator. The parameter η accounts for the anharmonicity of the qubit energy levels, with its value selected at the design stage. In our simulations we fixed $\eta = 0.2$ GHz (approximately $8.3 \cdot 10^{-7}$ eV), a typical value for transmon devices [21, 15]. The anharmonicity η can’t be controlled by electromagnetic signals. The terms $F_j(t)$ and $\psi_j(t)$ correspond to the amplitudes and phases of the microwave electromagnetic signals used to drive the j -th qubit state. Since the Hamiltonian is defined in a rotating frame of reference, in the laboratory frame of reference the drive control parameters $F_j(t)$ acts as an envelope for a sinusoidal carrier oscillating at the qubit resonant frequency [21, 15]. Lastly the term $g(t)$ accounts for qubit-qubit coupling, and it is controllable through an external magnetic flux [30]. The simulated gates require implementation times in the order of tens of nanoseconds; accordingly, the order of magnitude of the energy carried by control signals is GHz (approximately 10^{-6} eV).

In order to simplify both the Hamiltonian and the control signals, without loss of generality we

impose:

$$\psi_j(t) = 0, \quad \forall j. \quad (7)$$

Consequently, the system Hamiltonian can be rewritten as:

$$\begin{aligned} \hat{H}_{BH} = \sum_{j=1}^2 & \left[\delta_j(t) \hat{n}_j + \frac{\eta}{2} \hat{n}_j (\hat{n}_j - 1) + \right. \\ & + i(\hat{a}_j - \hat{a}_j^\dagger) F_j(t) \left. + \right. \\ & + g(t)(\hat{a}_1 \hat{a}_2^\dagger + \hat{a}_2 \hat{a}_1^\dagger) \left. \right]. \end{aligned} \quad (8)$$

We show that, even with such constraints, we have been able to implement all quantum gates of the chosen universal set. All the other terms with time dependence in (8) represent control parameters that we optimized through CRAB in order to implement the desired gates.

3. Optimizations Setup

We carried out the optimizations using Qutip’s CRAB implementation to define the control parameters of the Hamiltonian (8), using 10 sinusoidal and 10 cosinusoidal randomized basis functions for each parameter. All our optimizations adopt $\Gamma_j^0(t) = 1$ as initial pulse guess; therefore, we can reformulate the optimization problem in (2) as $\Gamma_j^{CRAB}(t) = G_j(t)$. In case an experimental setup needs control signals with a constrained envelope, the initial pulse guess can introduce the required constraints in the optimization process.

As cost functional for our optimizations [32] we set the gate infidelity. The mathematical definition of the adopted gate infidelity (from now on infidelity) is as follows:

$$I = 1 - \frac{1}{d^2} |\text{Tr}(\hat{U}_{\text{target}}^\dagger \hat{U}(T))|, \quad (9)$$

where d corresponds to the dimension of the Hilbert space, where the operators $\hat{U}(T)$ and \hat{U}_{target} act, $\hat{U}(T)$ refers to the solution of the time-dependent Schrödinger equation up to time T , with Hamiltonian (8), and \hat{U}_{target} is the target gate. We fixed the gate implementation time at $T = 40$ ns, a value above the quantum speed limit for this type of systems [33, 34, 35], and in line with state-of-the-art implementation times [36]. The infidelity (9) quantified how much the gate applied to our system via control pulses deviated from the ideal gate under investigation.

Non-computational energy levels of transmon qubits represent an important non-ideality in experimental gate implementations [27]. These extra levels can be exploited to implement fast and reliable gates [15], yet we need to avoid unwanted qubit leakages from computational to non-computational energy levels. We account for this non-ideality by approximating an hardware qubit via a three-level quantum system, interacting via a truncated version of the Hamiltonian (8). We simulated a three-level subspace since for transmon qubits the third energy level represents the most dominant contribution to leakages outside the computational subspace defined by the two lowest energy levels [16]. Moreover, simulating qubits with more than three energy levels significantly increases the simulation cost in Qutip, leading to unpractical optimization times. In our approximation, the first and second energy levels correspond to the qubit computational states $|0\rangle$ and $|1\rangle$, respectively, while the third level corresponds to the non-computational state $|2\rangle$ [16, 18]. All gates matrices have been reshaped in order to act on this three-level subspace. We put no constraints on how $\hat{U}(T)$ acts on the third energy level since the population of this non-computation state is an imperfection itself. Accordingly, to calculate the infidelity, we firstly discard the non-computational energy levels from $\hat{U}(T)$, and then compute Eq. (9) with the ideal two-level target gate U_{target} . This approach has the advantage of reducing the numerical complexity of the optimization.

4. Optimal Control Solutions Analysis

In this section we present the solutions of the different numerical experiments performed with the CRAB algorithm. We considered a gate successfully implemented when its infidelity was minimized below the threshold, set at 10^{-2} . We decided to adopt this threshold value since it approximates the infidelity magnitude of the best performing gates implemented on experimental transmon systems [37, 38, 39]. Furthermore, we gathered 30 different optimal control solutions for each gate of the chosen universal set in order to benchmark the average and best performances, as well as to weigh lucky gate implementations. All optimization attempts have been able to define the control solutions at the first try with our target infidelity of 10^{-2} . The average and the minimum infidelities that we obtained are shown in Table 1.

| | Average Infidelity | Minimum Infidelity |
|----------|------------------------|------------------------|
| CNOT | $9.9930 \cdot 10^{-3}$ | $9.9577 \cdot 10^{-3}$ |
| Hadamard | $9.9944 \cdot 10^{-3}$ | $9.9742 \cdot 10^{-3}$ |
| phase | $9.9922 \cdot 10^{-3}$ | $9.9513 \cdot 10^{-3}$ |
| $\pi/8$ | $9.9938 \cdot 10^{-3}$ | $9.9290 \cdot 10^{-3}$ |

Table 1: Average and minimum infidelities with 30 different optimal control solutions.

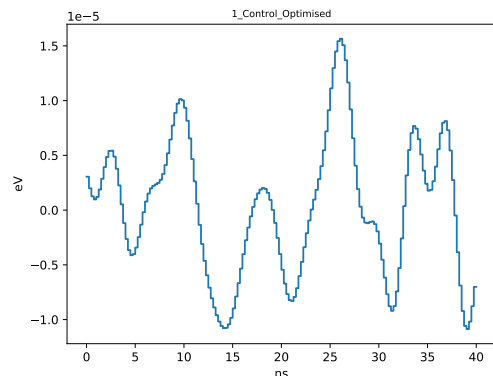


Figure 1: Amplitude $F_2(t)$ to implement a CNOT gate via the transmon Hamiltonian Eq. (8).

The control signals that compose one of the 30 optimal control solutions that implement the CNOT gate are shown in Figures 1, 2 and 3. This control solution has an infidelity of $9.9982 \cdot 10^{-3}$. Fig. 1 shows the profile of the amplitude $F_j(t)$ from Eq. (8) on the target qubit $j = 2$. Fig. 2 shows the profile of the control qubit detuning $\delta_1(t)$, while Fig. 3 shows the profile of the qubit-qubit coupling $g(t)$. Figs. 4, 5 and 6 show the spectra obtained by FFT analysis of the optimized control signals showed in Figure 1, 2 and 3, respectively.

In our theoretical approach we considered some of the main sources of problems and non-idealities that arise in experimental setups. In particular, we simulated the noise carried by control signals and the distortion that affects their spectra. The noise that we introduced on control signals is Gaussian and white, and can be considered as a simple approximation of stochastic noise sources affecting qubits [21, 15], such as the noise leaking from control electronics and the noise generated by the quantum hardware itself. There are also other types of noise affecting solid-state systems, and not considered in this work; in particular, $1/f$ noise sources are among the most important causes of decoher-

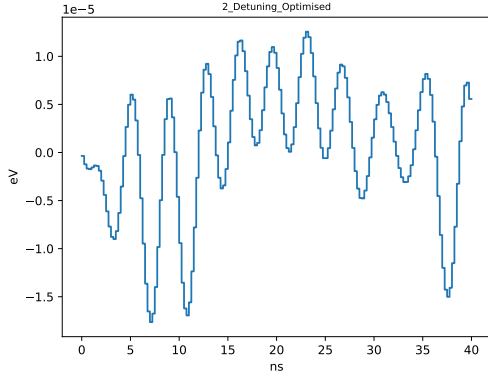


Figure 2: Detuning $\delta_1(t)$ to implement a CNOT gate via the transmon Hamiltonian Eq. (8).

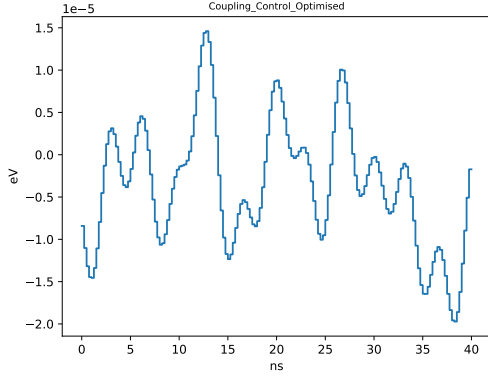


Figure 3: Coupling $g(t)$ to implement a CNOT gate via the transmon Hamiltonian Eq. (8).

ence in this kind of quantum systems [40, 41, 42].

The following equation describes the inclusion of noise in control signals:

$$\begin{aligned}\Gamma_j^{\text{noise}}(t) &= \Gamma_j^{\text{CRAB}}(t) + \Delta_j^{\text{noise}}(t) \\ &= G_j(t) + \Delta_j^{\text{noise}}(t) .\end{aligned}\quad (10)$$

The parameters $\Delta_j^{\text{noise}}(t)$ correspond to a time dependent white noise. To evaluate the noise resilience of existing optimal control solutions, we superimposed $\Delta_j^{\text{noise}}(t)$ to the optimized control signals [23]. We considered the noise tolerable by a control solution when 30 different noise realizations $\Delta_j^{\text{noise}}(t)$ with a guessed standard deviation $\sigma_{\Delta^{\text{noise}}}$ were able to give 30 consecutive gate implementations with an infidelity below 10^{-2} . In order to define $\sigma_{\Delta^{\text{noise}}}$, our algorithm proceeded by reducing it with -1 dB steps starting from 0.1 GHz (approx-

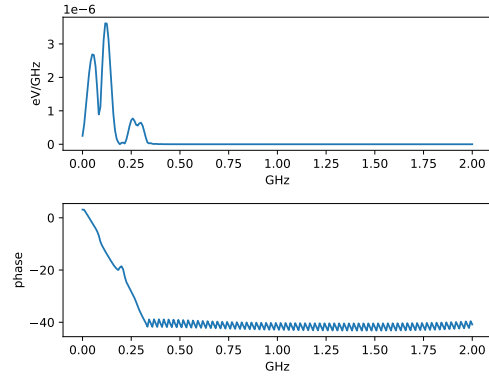


Figure 4: Fourier spectrum of the control signal $F_2(t)$ shown in Fig. 1.

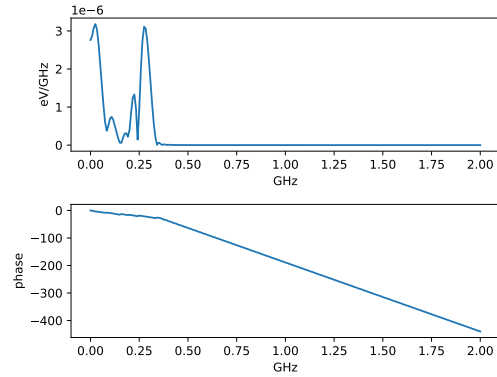


Figure 5: Fourier spectrum of the control signal $\delta_1(t)$ shown in Fig. 2.

imately $4.1 \cdot 10^{-7}$ eV), until the noise was tolerable by the tested control solution. We repeated this test for each of the 30 optimal control solutions that implement each of the gates of the universal set. Following the above definition, we call $\sigma_{\Delta^{\text{noise}}}^{\text{tol}}$ as the maximum tolerated value of $\sigma_{\Delta^{\text{noise}}}$. The $\sigma_{\Delta^{\text{noise}}}^{\text{tol}}$ of all the simulated gates are shown in Table 2. We found that, counter-intuitively, the introduction of noise for some given standard deviation levels improved the optimization performances to some extent. This finding is at presently outside the scope of this work, although a similar behavior was observed with parametric quantum circuits [43]; it will be further investigated in the future. Fig. 7 shows how $\sigma_{\Delta^{\text{noise}}}$ affects the infidelity of a CNOT gate, implemented through the optimized control signals shown in Figure 1, 2 and 3.

In order to account for the problems caused by

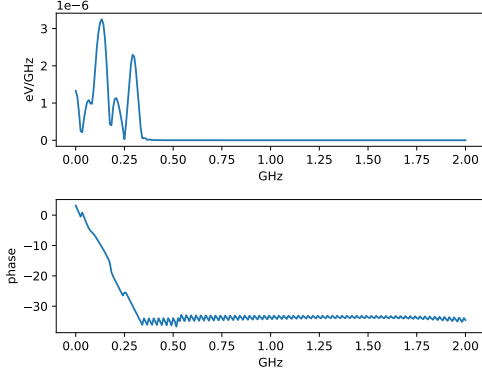


Figure 6: Fourier spectrum of the control signal $g(t)$ shown in Fig. 3.

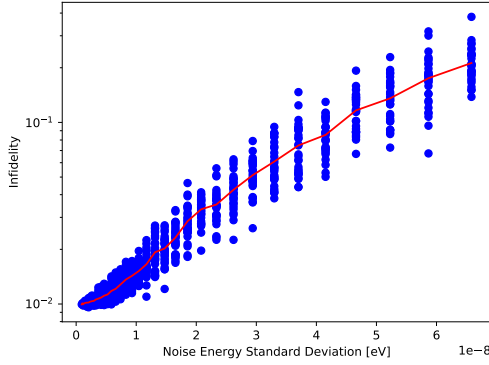


Figure 7: White noise standard deviation $\sigma_{\Delta^{noise}}$ versus gate infidelity of a CNOT gate implementation.

control signal distortions, we have also perturbed the basis coefficients of the optimal control solutions. Such perturbation can be considered as an approximation of systematic noise sources affecting control signals [21, 15], for example, the spectral distortion introduced by digital to analog conversions, transport mediums (e.g. wires and striplines) and undesired couplings with the quantum chip physical structure. The following equation describes the inclusion of the perturbation in

| | Average White Noise | Maximum White Noise |
|----------|-------------------------|-------------------------|
| CNOT | $1.52 \cdot 10^{-8}$ eV | $1.93 \cdot 10^{-8}$ eV |
| Hadamard | $1.55 \cdot 10^{-8}$ eV | $2.38 \cdot 10^{-8}$ eV |
| phase | $1.54 \cdot 10^{-8}$ eV | $1.96 \cdot 10^{-8}$ eV |
| $\pi/8$ | $1.54 \cdot 10^{-8}$ eV | $2.10 \cdot 10^{-8}$ eV |

Table 2: White noise standard deviations $\sigma_{\Delta^{noise}}$ tolerated by the system when simulating different universal gates.

the basis coefficients of an optimal control solution:

$$\begin{aligned}
\Gamma_j^{\text{dist.}}(t) &= \Gamma_j^{\text{CRAB}}(t) + \Delta_j^{\text{dist.}}(t) \\
&= \Gamma_j^{\text{CRAB}}(t) + \sum_{k=1}^{N_c} \Delta_j^k g_j^k(\omega_j^k t) \\
&= G_j(t) + \sum_{k=1}^{N_c} \Delta_j^k g_j^k(\omega_j^k t) \\
&= \sum_{k=1}^{N_c} (c_j^k + \Delta_j^k) g_j^k(\omega_j^k t) .
\end{aligned} \tag{11}$$

The parameters Δ_j^k superimpose a random perturbation, on the j -th coefficient c_j^k of an optimized control signal. To evaluate the resilience of the optimal control solutions against distortion, we superimpose Δ_j^k to the coefficients of basis functions of its control signals [23]. We considered the spectral distortion tolerable by a control solution when 30 different realizations of a random distortion $\Delta_j^{\text{dist.}}(t)$ with a guessed standard deviation σ_{Δ} for its coefficients Δ_j^k were able to give 30 consecutive gate implementations with an infidelity below 10^{-2} . In order to define σ_{Δ} , our algorithm proceeded by reducing it with -1 dB steps, starting from 0.1 GHz (approximately $4.1 \cdot 10^{-7}$ eV), until the disturbance was tolerable by the tested control solution. We repeated this test for each of the 30 optimal control solutions that implement each of the gates of the universal set. Following the above definition, we call $\sigma_{\Delta}^{\text{tol.}}$ as the maximum tolerated value of σ_{Δ} . The $\sigma_{\Delta}^{\text{tol.}}$ of all the simulated gates are shown in Table 3. Even during this test we observed that some levels of perturbation of basis coefficients slightly improved the optimization performances. Fig. 8 shows how σ_{Δ} affects the infidelity of a CNOT gate implemented through the optimized control signals shown in Figure 1, 2 and 3.

We now introduce a qualitative reasoning to compare how noise and perturbations on the coefficients affect the optimal control solutions. The scope of

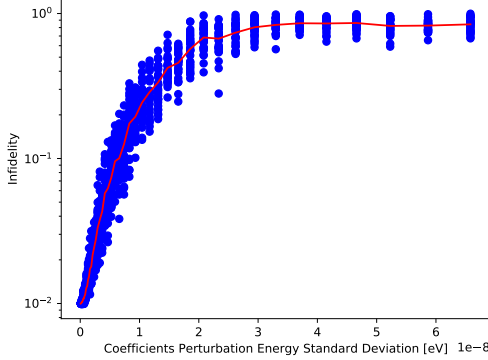


Figure 8: Perturbation of a coefficient standard deviation (i.e. σ_Δ) versus gate infidelity of a CNOT gate implementation.

| | Average Coeff. Pert. | Maximum Coeff. Pert. |
|----------|-------------------------|-------------------------|
| CNOT | $1.09 \cdot 10^{-9}$ eV | $1.87 \cdot 10^{-9}$ eV |
| Hadamard | $1.00 \cdot 10^{-9}$ eV | $2.01 \cdot 10^{-9}$ eV |
| phase | $1.11 \cdot 10^{-9}$ eV | $1.76 \cdot 10^{-9}$ eV |
| $\pi/8$ | $1.03 \cdot 10^{-9}$ eV | $1.83 \cdot 10^{-9}$ eV |

Table 3: White noise standard deviations σ_Δ tolerated by the system when simulating different universal gates.

the comparison is to find if one of the two disturb sources can be better tolerated by control signals. Distortions in the frequency domain can be used to construct a time dependent distortion signal, mathematically defined as:

$$\Delta_j^{\text{dist.}}(t) = \sum_{k=1}^{N_c} \Delta_j^k g_j^k(\omega_j^k t) . \quad (12)$$

All coefficient perturbations Δ_j^{1,\dots,N_c} have a normal distribution with zero expectation value and standard deviation equal to σ_Δ . Since g_j^k correspond to sinusoidal and cosinusoidal functions, it is possible to observe that:

$$\Delta_j^{\text{dist.}}(t) = \sum_{k=1}^{N_c} \Delta_j^k g_j^k(\omega_j^k t) \leq \sum_{k=1}^{N_c} |\Delta_j^k| \simeq N_c \cdot \mu , \quad (13)$$

where in the last approximation we have replaced the stochastic coefficient $|\Delta_j^k|$ with their mean μ . Since $|\Delta_j^k|$ are identically distributed and follow a half-normal distribution, we get

$$\mu = \sigma_\Delta \cdot \sqrt{\frac{2}{\pi}} . \quad (14)$$

The distortion $\Delta_j^{\text{dist.}}(t)$ has the characteristic of a periodic source that lies in the band of control signals, and its energy is approximately contained within $\mu^{\text{dist.}} = N_c \cdot \mu$. The average tolerated $\sigma_\Delta^{\text{tol.}}$ that we obtained for 30 implementations of a CNOT gate is $\sigma_\Delta^{\text{tol.}} \simeq 1.09 \cdot 10^{-9}$ eV. From Eq.(14) we obtain $\mu \simeq 0.87 \cdot 10^{-9}$ eV for a single perturbation of a basis coefficient. Since we have control signals with $N_c = 20$ coefficients (10 for sinusoidal basis functions and 10 for cosinusoidal basis functions), from Eq.(13) we obtain $\mu^{\text{dist.}} \simeq 1.74 \cdot 10^{-8}$ eV. The periodic source $\Delta_j^{\text{dist.}}(t)$ should have an energy amplitude less than $\mu^{\text{dist.}}$ to not invalidate gate implementations. Following a similar reasoning, we can define a bound μ^{noise} on the energy amplitude of the white noise $\Delta_j^{\text{noise}}(t)$. As before, we find $\mu^{\text{noise}} = \sigma_{\Delta^{\text{noise}}} \cdot \sqrt{2/\pi}$. The average tolerated $\sigma_{\Delta^{\text{noise}}}^{\text{tol.}}$ that we obtained for 30 implementations of a CNOT gate is $\sigma_{\Delta^{\text{noise}}}^{\text{tol.}} \simeq 1.52 \cdot 10^{-8}$ eV. Hence we obtain that $\mu^{\text{noise}} \simeq 1.21 \cdot 10^{-8}$ eV.

The comparison of μ^{noise} and $\mu^{\text{dist.}}$ suggests that our optimal control solutions may tolerate a little better the distortion that affect their spectra than the white noise. This result holds for all gates of the simulated universal set as is possible to observe comparing the two disturb sources using the data from Table 2 and Table 3.

As is possible to observe from Table 1, the obtained infidelities when no disturbances are superimposed on control signals are slightly below the target threshold. As a consequence, the optimal control solutions disturbed by noise and spectral distortion tend to easily exceed the infidelity threshold. The aforementioned consideration and the choice to set the same threshold for the ideal and the disturbed gate implementations probably lead to tolerable noise and spectral distortion levels smaller than necessary. Allowing a tolerable error on the infidelity of disturbed gate implementations could help to define less strict tolerable noise and spectral distortion levels.

5. Conclusions

In this letter we have benchmarked the robustness in the implementation of quantum gates in a two-transmon system, where each transmon is approximated as a three-level system with a single non-computational state. Optimal control signals to implement different gates from a universal set were obtained using the CRAB algorithm, and dif-

ferent sources of electronic imperfections were modeled as signal noise and spectral distortions. We report that we have been able to implement all gates from the chosen universal set with an infidelity below 10^{-2} and with a fixed control time $T = 40$ ns, exploiting the CRAB optimization method. We also note that all optimization attempts have been able to define the control solutions at the first try, in spite of the errors caused by non-computational energy levels.

We observed that to obtain a proper gate implementation it is mandatory to minimize noise and spectral distortion in control signals. We found the introduction of noise in control signals seems to be slightly less tolerated than spectral distortion. In future studies, it may be interesting to test the resilience of the optimal control solutions against colored noises and spectral distortion with different weight for each basis coefficient. The numerical analysis allowed us to define empirical energy bounds for the Gaussian white noise (i.e. $\sigma_{\Delta\text{noise}}$) and the spectral distortion (i.e. σ_{Δ}) that can be tolerated by optimal control solutions [23, 22, 24].

We also observed that some optimal control signals showed a significantly higher tolerance to disturbances. For some gates we observed ~ 3 dB between $\sigma_{\Delta\text{noise}}$ of the average and the best performing gate implementations with noisy signals (see Table 2). Similarly, for perturbations in the coefficients we observed ~ 6 dB between σ_{Δ} of the average and the best performing gate implementations (see Table 3). It could be interesting to study whether the optimal control solutions that tolerated higher disturbances share some common characteristics. In case their best behavior could be treated deterministically, it may be possible to evolve CRAB to directly synthesize control solutions, capable of sustaining the typical disturbances of a target experimental system.

References

- [1] R. P. Feynman, Simulating physics with computers, in: Feynman and computation, CRC Press, 2018, pp. 133–153.
- [2] M. A. Nielsen, I. Chuang, Quantum computation and quantum information (2002).
- [3] C. Brif, R. Chakrabarti, H. Rabitz, Control of quantum phenomena: past, present and future, New Journal of Physics 12 (7) (2010) 075008.
- [4] S. J. Glaser, U. Boscain, T. Calarco, C. P. Koch, W. Köckenberger, R. Kosloff, I. Kuprov, B. Luy, S. Schirmer, T. Schulte-Herbrüggen, et al., Training schrödinger’s cat: quantum optimal control, The European Physical Journal D 69 (12) (2015) 1–24.
- [5] D. d’Alessandro, Introduction to quantum control and dynamics, CRC press, 2007.
- [6] J. L. O’Brien, A. Furusawa, J. Vučković, Photonic quantum technologies, Nature Photonics 3 (12) (2009) 687–695.
- [7] V. Jurdjevic, J. Velimir, V. Đurđević, Geometric control theory, Cambridge university press, 1997.
- [8] T. Caneva, T. Calarco, S. Montangero, Chopped random-basis quantum optimization, Physical Review A 84 (2) (2011) 022326.
- [9] N. Rach, M. M. Müller, T. Calarco, S. Montangero, Dressing the chopped-random-basis optimization: A bandwidth-limited access to the trap-free landscape, Physical Review A 92 (6) (2015) 062343.
- [10] M. M. Müller, R. S. Said, F. Jelezko, T. Calarco, S. Montangero, One decade of quantum optimal control in the chopped random basis, arXiv preprint arXiv:2104.07687 (2021).
- [11] N. Khaneja, T. Reiss, C. Kehlet, T. Schulte-Herbrüggen, S. J. Glaser, Optimal control of coupled spin dynamics: design of nmr pulse sequences by gradient ascent algorithms, Journal of magnetic resonance 172 (2) (2005) 296–305.
- [12] L. Banchi, G. E. Crooks, Measuring analytic gradients of general quantum evolution with the stochastic parameter shift rule, Quantum 5 (2021) 386.
- [13] M. H. Devoret, R. J. Schoelkopf, Superconducting circuits for quantum information: an outlook, Science 339 (6124) (2013) 1169–1174.
- [14] G. Wendin, Quantum information processing with superconducting circuits: a review, Reports on Progress in Physics 80 (10) (2017) 106001.
- [15] P. Krantz, M. Kjaergaard, F. Yan, T. P. Orlando, S. Gustavsson, W. D. Oliver, A quantum engineer’s guide to superconducting qubits, Applied Physics Reviews 6 (2) (2019) 021318.
- [16] P. Rebentrost, F. K. Wilhelm, Optimal control of a leaking qubit, Physical Review B 79 (6) (2009) 060507.
- [17] A. Spörl, T. Schulte-Herbrüggen, S. Glaser, V. Bergholm, M. Storz, J. Ferber, F. Wilhelm, Optimal control of coupled josephson qubits, Physical Review A 75 (1) (2007) 012302.
- [18] M. Werninghaus, D. J. Egger, F. Roy, S. Machnes, F. K. Wilhelm, S. Filipp, Leakage reduction in fast superconducting qubit gates via optimal control, npj Quantum Information 7 (1) (2021) 1–6.
- [19] P. Watts, J. Vala, M. M. Müller, T. Calarco, K. B. Whaley, D. M. Reich, M. H. Goerz, C. P. Koch, Optimizing for an arbitrary perfect entangler. i. functionals, Physical Review A 91 (6) (2015) 062306.
- [20] J. Koch, M. Y. Terri, J. Gambetta, A. A. Houck, D. I. Schuster, J. Majer, A. Blais, M. H. Devoret, S. M. Girvin, R. J. Schoelkopf, Charge-insensitive qubit design derived from the cooper pair box, Physical Review A 76 (4) (2007) 042319.
- [21] J. C. Bardin, D. Sank, O. Naaman, E. Jeffrey, Quantum computing: An introduction for microwave engineers, IEEE Microwave Magazine 21 (8) (2020) 24–44.
- [22] S. Lloyd, S. Montangero, Information theoretical analysis of quantum optimal control, Physical review letters 113 (1) (2014) 010502.
- [23] S. Kallush, M. Khasin, R. Kosloff, Quantum control with noisy fields: computational complexity versus sen-

- sitivity to noise, *New Journal of Physics* 16 (1) (2014) 015008.
- [24] M. M. Müller, S. Gherardini, T. Calarco, S. Montangero, F. Caruso, Information theoretical limits for quantum optimal control solutions: Error scaling of noisy channels, *arXiv preprint arXiv:2006.16113* (2020).
 - [25] J. M. Chow, J. M. Gambetta, A. D. Corcoles, S. T. Merkel, J. A. Smolin, C. Rigetti, S. Poletto, G. A. Keefe, M. B. Rothwell, J. R. Rozen, et al., Universal quantum gate set approaching fault-tolerant thresholds with superconducting qubits, *Physical review letters* 109 (6) (2012) 060501.
 - [26] J. Long, T. Zhao, M. Bal, R. Zhao, G. S. Barron, H.-s. Ku, J. A. Howard, X. Wu, C. R. H. McRae, X.-H. Deng, et al., A universal quantum gate set for transmon qubits with strong zz interactions, *arXiv preprint arXiv:2103.12305* (2021).
 - [27] E. Zahedinejad, J. Ghosh, B. C. Sanders, High-fidelity single-shot toffoli gate via quantum control, *Physical review letters* 114 (20) (2015) 200502.
 - [28] J. R. Johansson, P. D. Nation, F. Nori, Qutip: An open-source python framework for the dynamics of open quantum systems, *Computer Physics Communications* 183 (8) (2012) 1760–1772.
 - [29] J. A. Nelder, R. Mead, A simplex method for function minimization, *The computer journal* 7 (4) (1965) 308–313.
 - [30] Y. Chen, C. Neill, P. Roushan, N. Leung, M. Fang, R. Barends, J. Kelly, B. Campbell, Z. Chen, B. Chiaro, et al., Qubit architecture with high coherence and fast tunable coupling, *Physical review letters* 113 (22) (2014) 220502.
 - [31] M. Y. Niu, S. Boixo, V. N. Smelyanskiy, H. Neven, Universal quantum control through deep reinforcement learning, *npj Quantum Information* 5 (1) (2019) 1–8.
 - [32] P. Rembold, N. Oshnik, M. M. Müller, S. Montangero, T. Calarco, E. Neu, Introduction to quantum optimal control for quantum sensing with nitrogen-vacancy centers in diamond, *AVS Quantum Science* 2 (2) (2020) 024701.
 - [33] M. M. Taddei, B. M. Escher, L. Davidovich, R. L. de Matos Filho, Quantum speed limit for physical processes, *Physical review letters* 110 (5) (2013) 050402.
 - [34] N. Margolus, L. B. Levitin, The maximum speed of dynamical evolution, *Physica D: Nonlinear Phenomena* 120 (1-2) (1998) 188–195.
 - [35] K. Bhattacharyya, Quantum decay and the mandelstam-tamm-energy inequality, *Journal of Physics A: Mathematical and General* 16 (13) (1983) 2993.
 - [36] R. Barends, J. Kelly, A. Megrant, A. Veitia, D. Sank, E. Jeffrey, T. C. White, J. Mutus, A. G. Fowler, B. Campbell, et al., Superconducting quantum circuits at the surface code threshold for fault tolerance, *Nature* 508 (7497) (2014) 500–503.
 - [37] F. Arute, K. Arya, R. Babbush, D. Bacon, J. C. Bardin, R. Barends, R. Biswas, S. Boixo, F. G. Brandao, D. A. Buell, et al., Quantum supremacy using a programmable superconducting processor, *Nature* 574 (7779) (2019) 505–510.
 - [38] J. Kelly, R. Barends, B. Campbell, Y. Chen, Z. Chen, B. Chiaro, A. Dunsworth, A. G. Fowler, I.-C. Hoi, E. Jeffrey, et al., Optimal quantum control using randomized benchmarking, *Physical review letters* 112 (24) (2014) 240504.
 - [39] A. Kandala, K. Wei, S. Srinivasan, E. Magesan, S. Carnevale, G. Keefe, D. Klaus, O. Dial, D. McKay, Demonstration of a high-fidelity cnot gate for fixed-frequency transmons with engineered z z suppression, *Physical Review Letters* 127 (13) (2021) 130501.
 - [40] E. Paladino, Y. Galperin, G. Falci, B. Altshuler, $1/f$ noise: Implications for solid-state quantum information, *Reviews of Modern Physics* 86 (2) (2014) 361.
 - [41] S. Schlör, J. Lisenfeld, C. Müller, A. Bilmes, A. Schneider, D. P. Pappas, A. V. Ustinov, M. Weides, Correlating decoherence in transmon qubits: Low frequency noise by single fluctuators, *Physical review letters* 123 (19) (2019) 190502.
 - [42] S. Montangero, T. Calarco, R. Fazio, Robust optimal quantum gates for josephson charge qubits, *Physical review letters* 99 (17) (2007) 170501.
 - [43] L. Gentini, A. Cuccoli, S. Pirandola, P. Verrucchi, L. Banchi, Noise-resilient variational hybrid quantum-classical optimization, *Physical Review A* 102 (5) (2020) 052414.